Supporting Information for:

Synthesis of Organic HCl Salts via Mechanochemical Salification and their Characterization with $^{35/37}$Cl Solid-State NMR Spectroscopy

Zachary T. Dowdell[1,2], Peyton G. Osborn[1,2], Victoria K. Rash[3], Trisha S. Patel[1], Alexander M. Perez[1], Xinsong Lin[1], Sean T. Holmes[1,2,*], and Robert. W. Schurko[1,2,†]

[1] Department of Chemistry and Biochemistry, Florida State University, Tallahassee, FL, 32306.

[2] National High Magnetic Field Laboratory, Tallahassee, FL 32310

[3] Department of Physics, University of Texas, Dallas, TX, 75080

[†]Deceased February 2026

*Author to whom correspondence should be addressed.

E-mail: sholmes2@fsu.edu

Contents

Table S1. ^{35}Cl SSNMR acquisition parameters at 18.8 T.

Material	Static/MAS (ν_{rot} in kHz)	Pulse Sequence [a]	No. Scans	Experimental Time (hr)	Recycle Delay (s)	Echo Length (μs) [b]	Echoes	Dwell Time (μs)	Spectral Width (kHz)	Time Domain Size	Pulse width [π/2] (μs)
NicH-Nic:H_2O	Static	QCPMG	6047	10.1	6.0	1000	30	2.0	250	17408	2.50
	MAS (15)	Bloch Decay	256	0.4	6.0	-	-	2.0	250	10240	2.50
NicH	Static	QCPMG	2048	2.8	5.0	750	35	1.0	500	31744	3.57
	MAS (20)	QCPMG	256	0.4	5.0	400	50	2.5	200	10240	12.50
IsoH-Iso:H_2O	Static	QCPMG	3848	4.3	4.0	300	66	1.0	500	30720	2.08
IsoH	Static	QCPMG	1024	1.7	6.0	300	66	2.0	250	14500	5.0
	MAS (15)	QCPMG	256	0.4	6.0	300	66	2.0	250	14336	5.0
PicH-Pic	Static	Hahn Echo	24280	4.5	1.5	-	1	5.0	100	1024	25.0
	MAS (10)	Hahn Echo	32	0.01	1.5	-	1	5.0	100	2048	25.0
PicH:H_2O	Static	QCPMG	2048	1.7	3.0	500	70	1.0	500	38912	5.0
PicH	Static	Hahn Echo	2560	2.8	4.0	-	1	2.5	200	2048	12.5
	MAS (15)	Bloch Decay	256	0.2	3.0	-	-	20.0	25	4096	12.5
NicAH	Static	WCPMG	16384	11.4	2.5	400	50	0.43	1153.8	65536	5.0
IsoAH	Static	QCPMG	4096	4.6	4.0	500	60	1.0	500	37888	2.5
PicAH-PicA	Static	QCPMG	20480	14.2	2.5	500	55	1.67	300	20480	3.57
PicAH:H_2O	Static	QCPMG	20480	11.4	2.0	300	66	1.67	300	12288	4.17
	MAS (19)	QCPMG	4096	2.3	2.0	300	40	2.0	250	20480	4.17
PicAH	Static	WCPMG	16384	18.2	4.0	300	75	0.67	750	49152	5.0
CaffH:H_2O	Static	QCPMG	5120	2.8	2.0	500	50	1.0	500	31744	5.0
	MAS (20)	QCPMG	512	0.4	3.0	500	45	2.0	250	14336	5.0
CaffH	Static	QCPMG	3840	4.3	4.0	400	70	1.0	500	35840	2.5
AcetH-Acet	Static	QCPMG	3504	3.9	4.0	500	55	2.0	250	17408	8.34
	MAS (20)	QCPMG	2048	1.1	2.0	750	45	2.0	250	14336	5.0
AcetH:H_2O	Static	Hahn Echo	8192	6.8	3.0	-	1	5.0	100	1024	5.0
	MAS (15)	Hahn Echo	1568	1.3	3.0	-	1	5.0	100	1024	5.0
AcetH-Acet:H_2O	Static	Hahn Echo	5120	4.3	3.0	-	1	5.0	100	1024	25.0
	MAS (10)	Bloch Decay	2048	1.7	3.0	-	-	5.0	100	2048	25.0

[a] Pulse sequences include Bloch decay (single 90° pulse), Hahn echo (90°–τ–180°–τ–acq), quadrupolar Carr-Purcell Meiboom-Gill (QCPMG), and wideband uniform-rate smooth truncation/CPMG (WURST-CPMG or WCPMG). These sequences used 8, 8, 16-, and 16-step phase cycles, respectively.
[b] The echo length is defined as the time between 180° pulses.

Table S2. ^{37}Cl SSNMR acquisition parameters at 18.8 T.

Material	Pulse Sequence [a]	No. Scans	Experimental Time (hr)	Recycle Delay (s)	Echo Length (μs) [b]	Echoes	Dwell Time (μs)	Spectral Width (kHz)	Time Domain Size	Pulse width [π/2] (μs)	Contact Time (ms)
NicH-Nic:H_2O	Hahn Echo	16384	9.1	2.0	-	1	2.5	200	2048	12.50	-
NicH	QCPMG	10240	14.2	5.0	800	35	1.0	500	32768	5.0	-
IsoH-Iso:H_2O	QCPMG	512	1.0	7.0	300	90	1.25	400	26624	3.57	-
IsoH	QCPMG	1024	1.1	5.0	1000	33	4.0	125	9216	8.33	-
PicH-Pic	QCPMG	20480	5.7	1.0	4000	9	10.0	50	3584	25.0	-
PicH:H_2O	QCPMG	4096	4.0	3.5	200	19	5.0	100	6144	12.5	-
PicH	Hahn Echo	4096	5.7	5.0	-	1	2.0	250	4096	25.0	-
NicAH	QCPMG	6784	6.6	3.5	600	60	1.25	400	30720	2.5	-
IsoAH	QCPMG	20480	17.1	3.0	700	28	2.0	250	10240	3.57	-
PicAH-PicA	QCPMG	12288	14.2	4.0	1000	28	2.0	250	16384	5.0	-
PicAH	WCPMG	14122	11.8	3.0	300	42	1.0	500	16384	5.0	-
CaffH:H_2O	QCPMG	8192	11.4	5.0	300	32	1.0	500	10240	5.0	-
CaffH	QCPMG	16384	13.6	3.0	500	50	1.25	400	20480	3.57	-
AcetH-Acet	QCPMG	4096	4.6	4.0	1000	17	2.0	250	10240	25	-
AcetH:H_2O	CP-CPMG	2048	0.3	2.5	1400	17	5.0	100	5120	25.0	20
AcetH-Acet:H_2O	QCPMG	5120	5.7	4.0	1400	6	10.0	50	3072	25.0	-

Table S3. pK_a values of various molecules.

Molecule	pK_a
Iso	3.61
Nic	3.35
Pic	2.10
NicA	2.08
IsoA	1.70
PicA	1.60

The pK_a values of these molecules are reported by Jellinek and Urwin, *1954*. See Ref. 123.

Table S4. Enthalpies of formation for the materials with known crystal structures.

Material	ΔH_f [a] (kJ mol^{-1})
NicH	−0.19
NicH-Nic:H_2O	0.05
Nic-Iso	10.60
IsoH	−10.69
PicH:H_2O	7.07
NicAH	−0.21
IsoAH	−0.21
PicAH	8.12
PicAH:H_2O	8.34

[a] Static lattice energies obtained from DFT-D2* calculations were computed from refinement of crystal structures of all known materials and starting reagents. Water is modelled as an isolated molecule.

Derived from the equation:

$$\Delta H_f = H_{product} - (AH_{educt}^{(1)} + BH_{educt}^{(2)} + CH_{water})$$

Example for **PicH:H_2O**:

$$\Delta H_f = H_{PicH:H2O} - (H_{Pic}^{(1)} + H_{HCl}^{(2)} + H_{water})$$

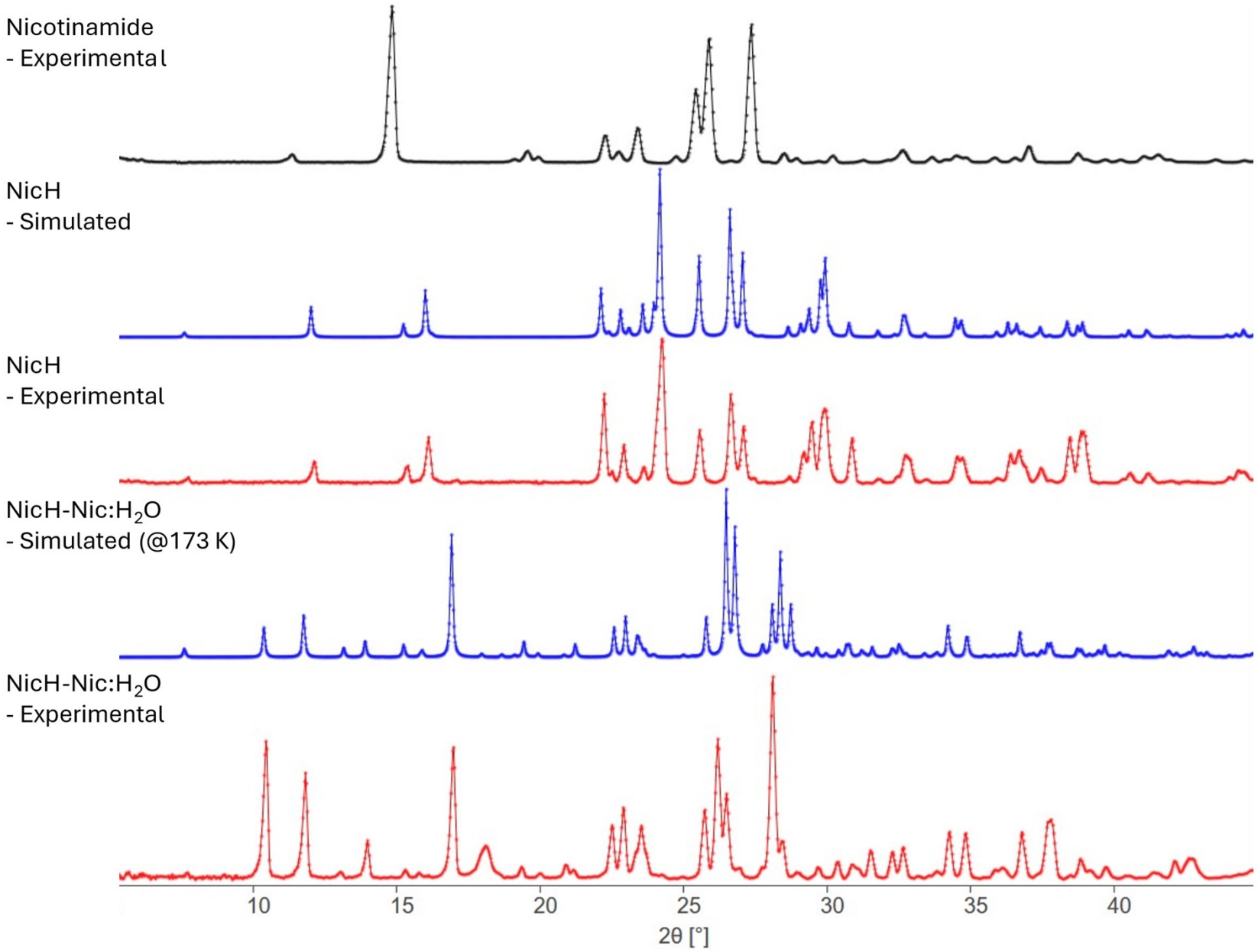

Fig. S1. Experimental and simulated PXRD patterns of nicotinamide, **NicH,** and **NicH-Nic:H_2O**.

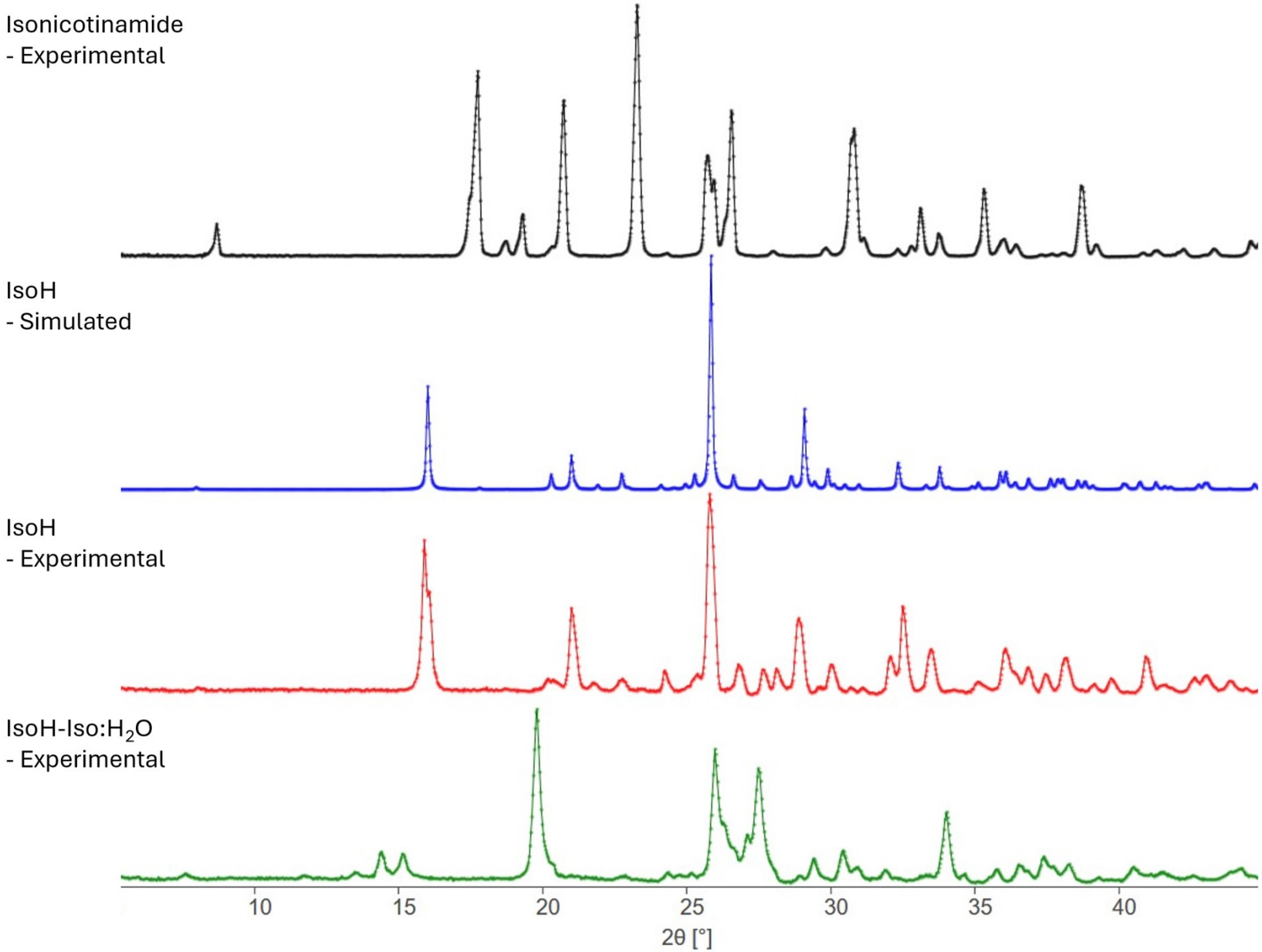

Fig. S2. Experimental and simulated PXRD patterns of isonicotinamide, **IsoH** and **IsoH-Iso:H_2O**.

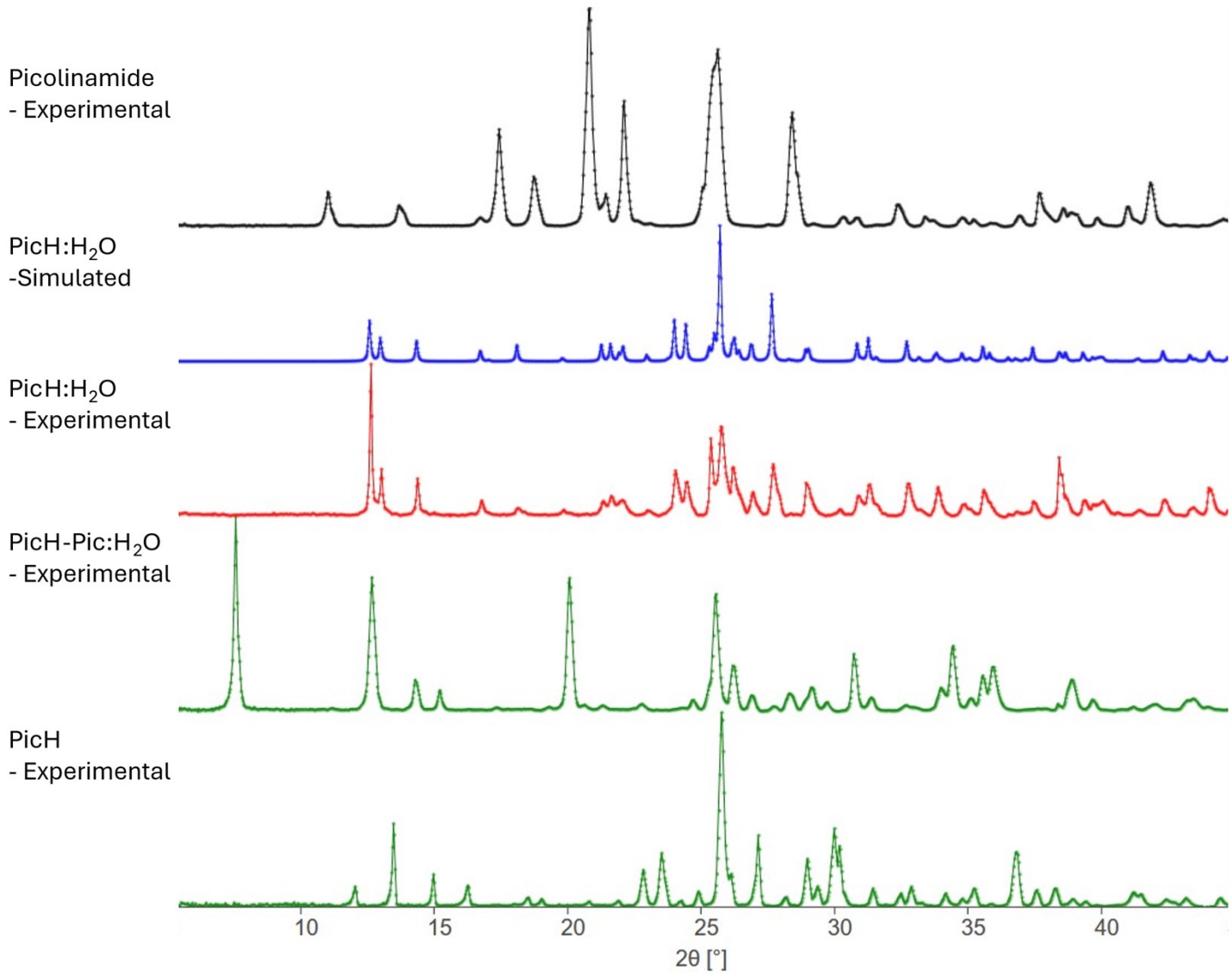

Fig. S3. Experimental and simulated PXRD patterns of picolinamide, **PicH:H_2O**, **PicH-Pic:H_2O**, and **PicH**.

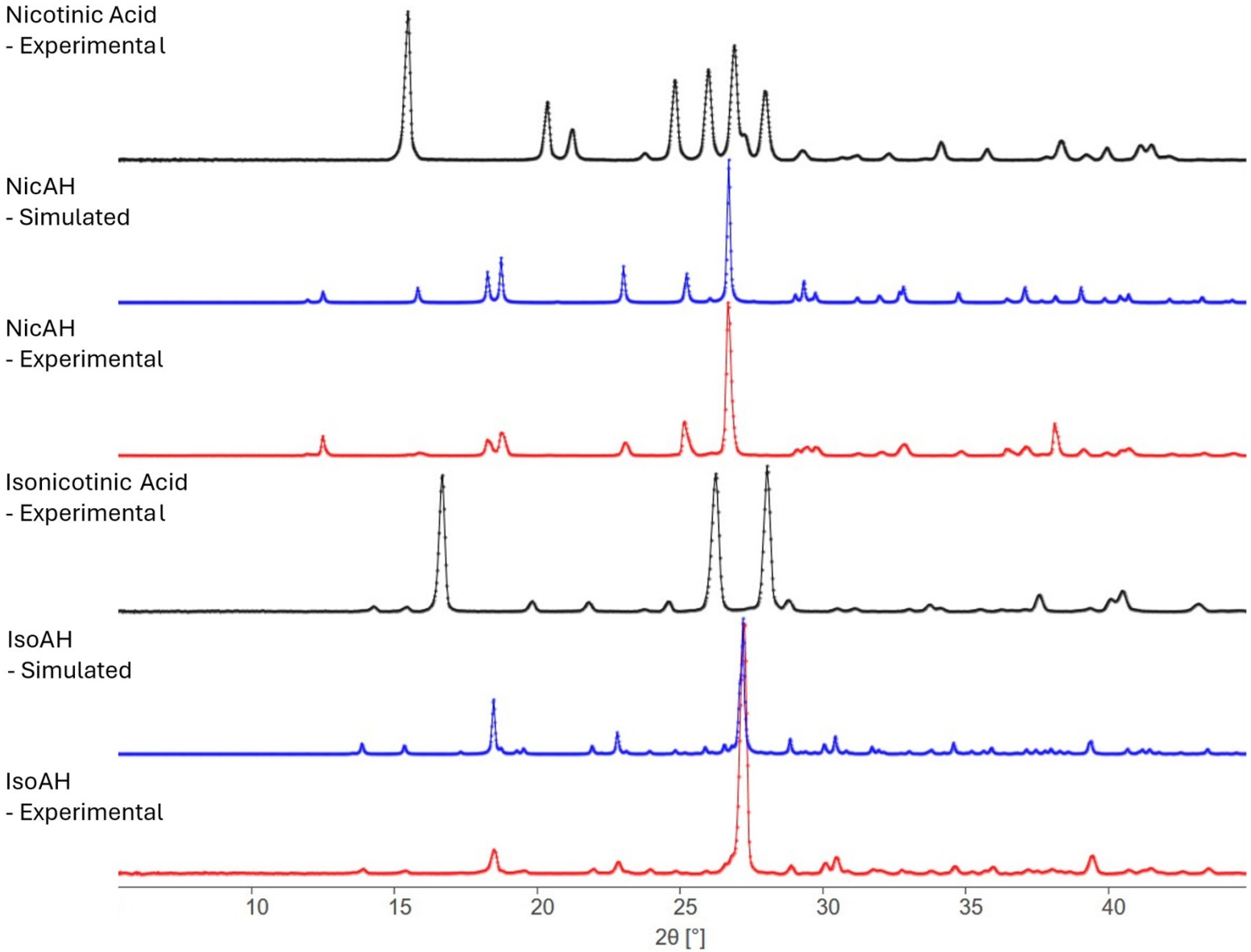

Fig. S4. Experimental and simulated PXRD patterns of nicotinic acid, isonicotinic acid, **NicAH**, and **IsoAH**.

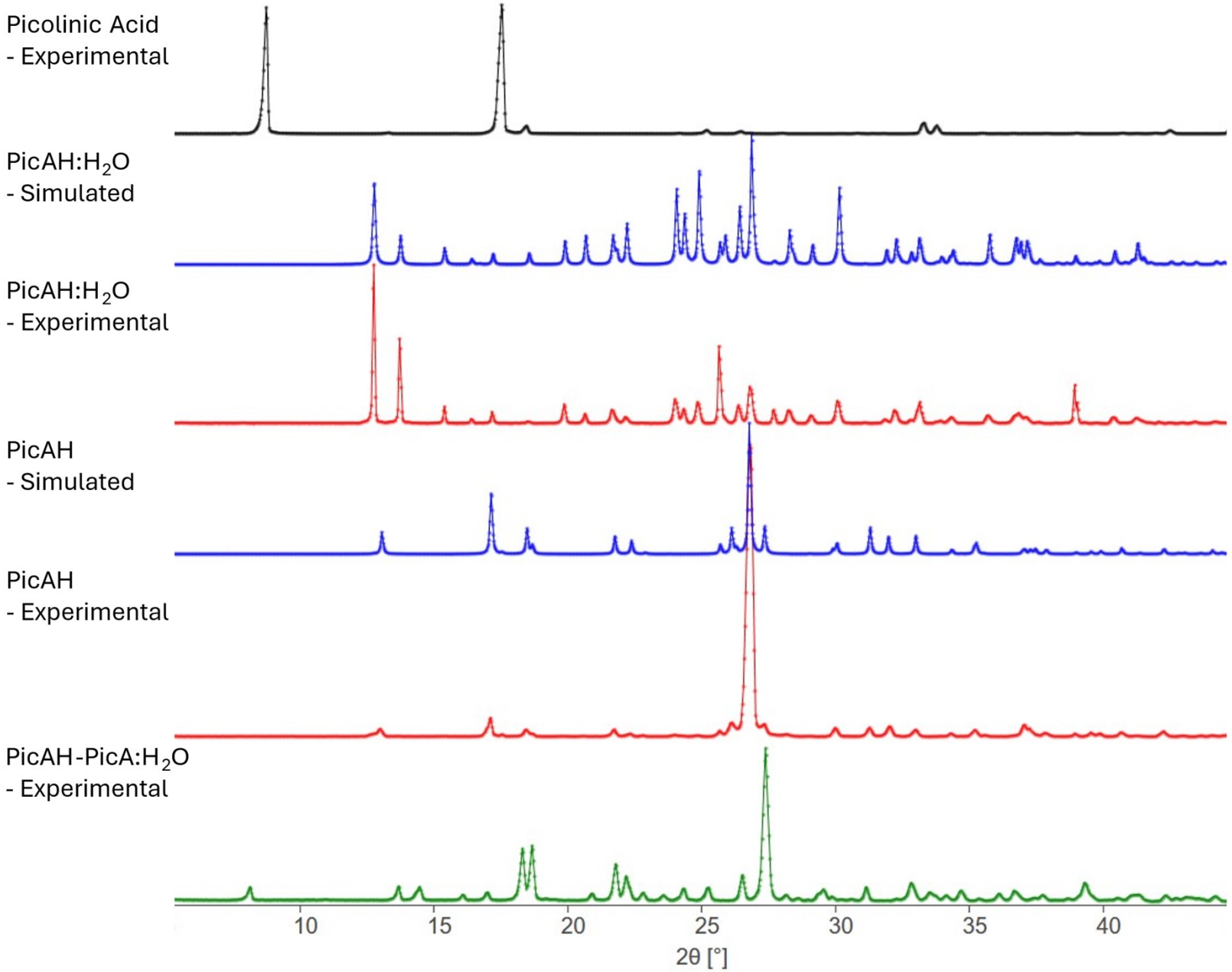

Fig. S5. Experimental and simulated PXRD patterns of picolinic acid, **PicAH:H_2O**, **PicAH** and **PicAH-PicA:H_2O**.

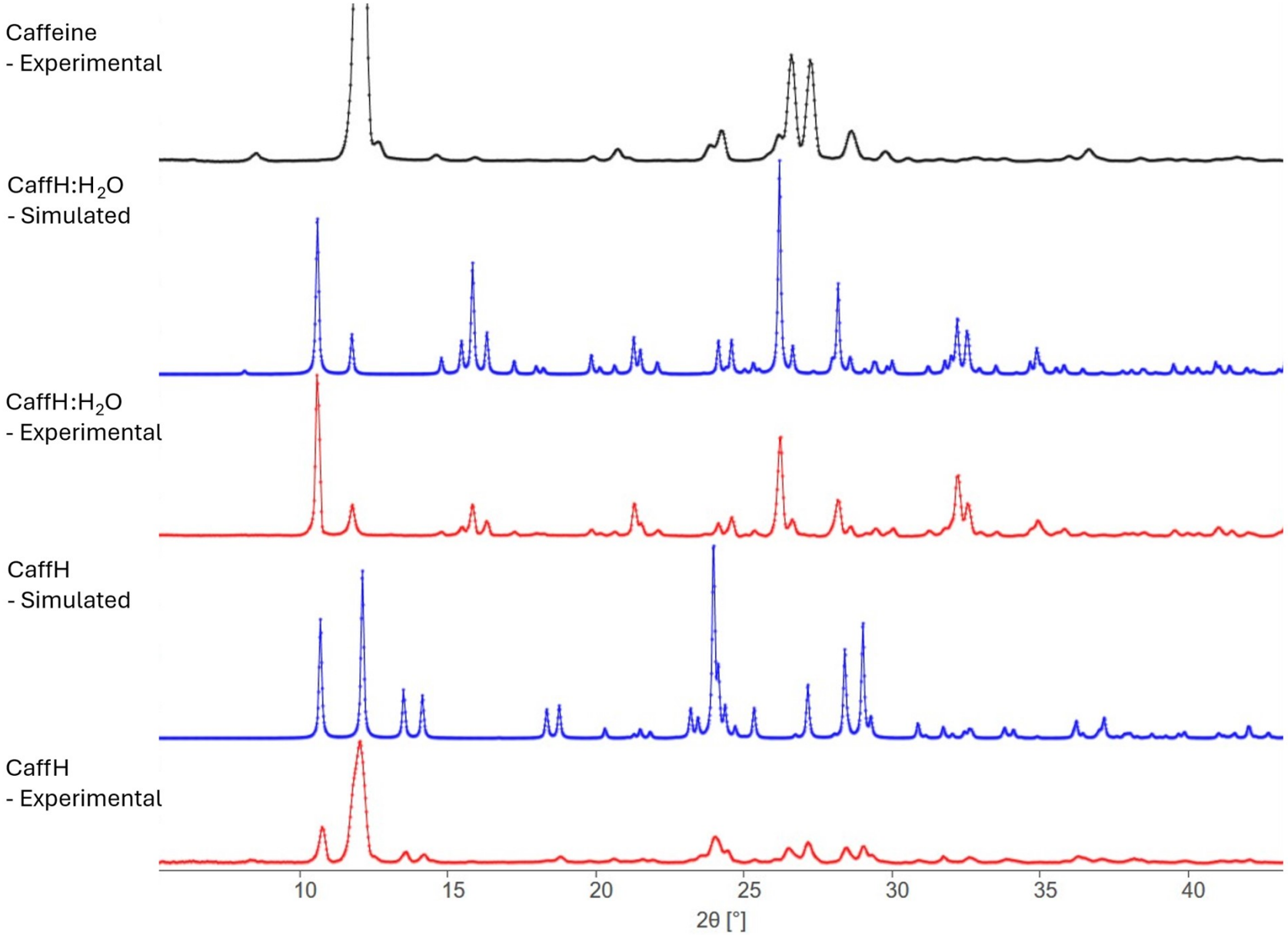

Fig. S6. Experimental and simulated PXRD patterns of caffeine, **CaffH:H_2O**, and **CaffH.**

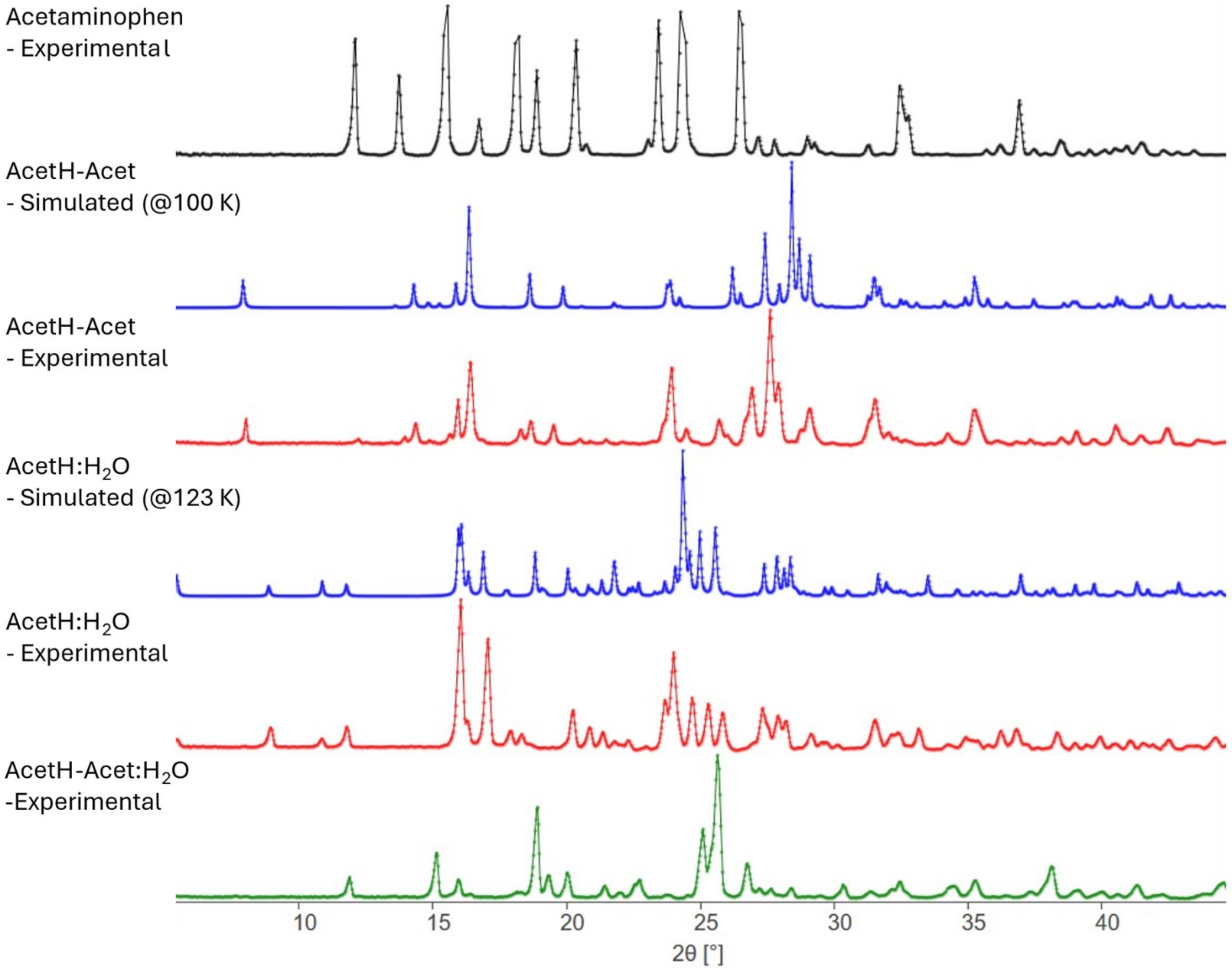

Fig. S7. Experimental and simulated PXRD patterns of acetaminophen, **AcetH-Acet**, **AcetH:H_2O**, **AcetH-Acet:H_2O**.

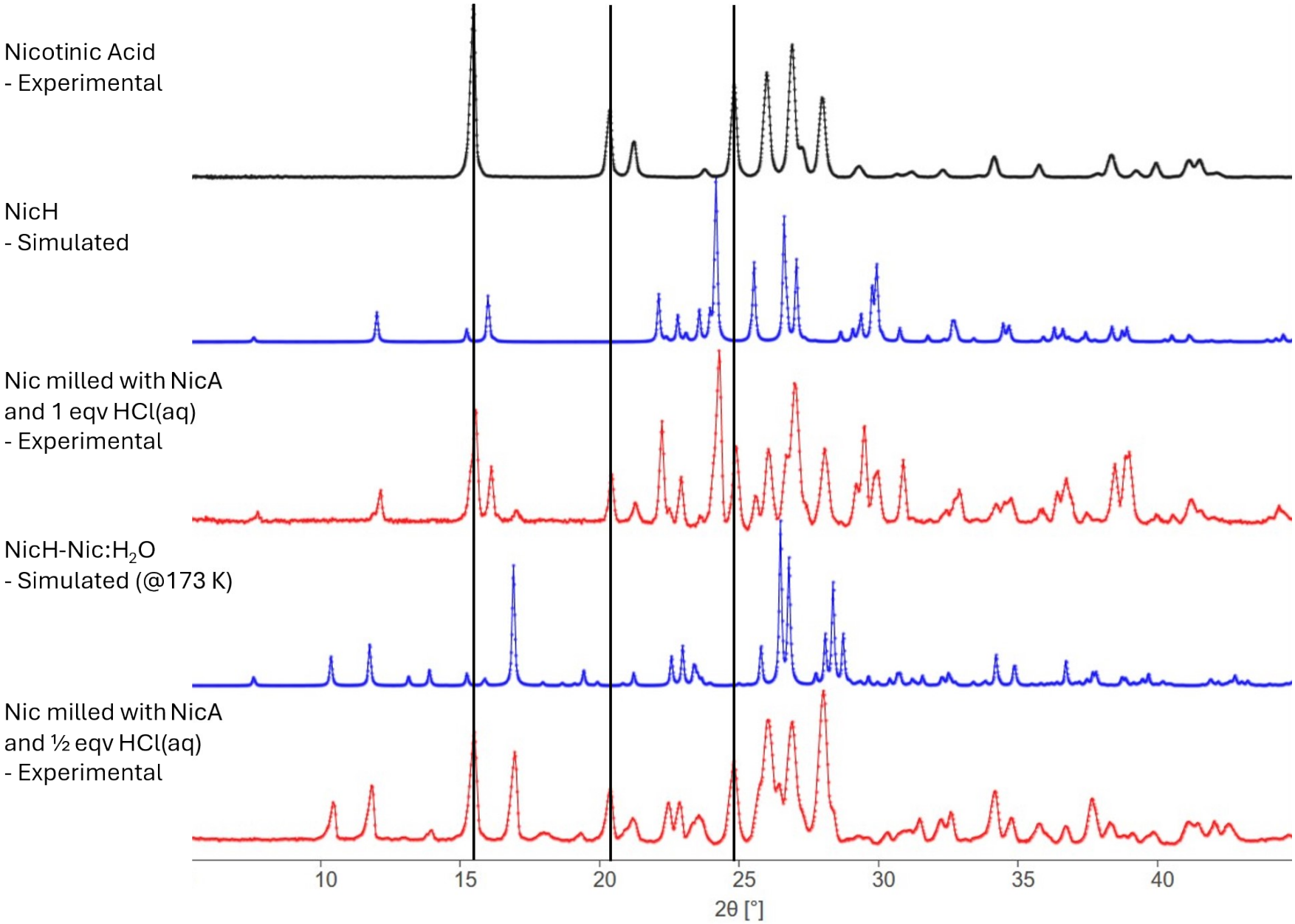

Fig. S8. PXRD patterns of **NicA**, **NicH**, and **NicH-Nic:H_2O** and competitive milling reactions between **Nic** and **NicA**.

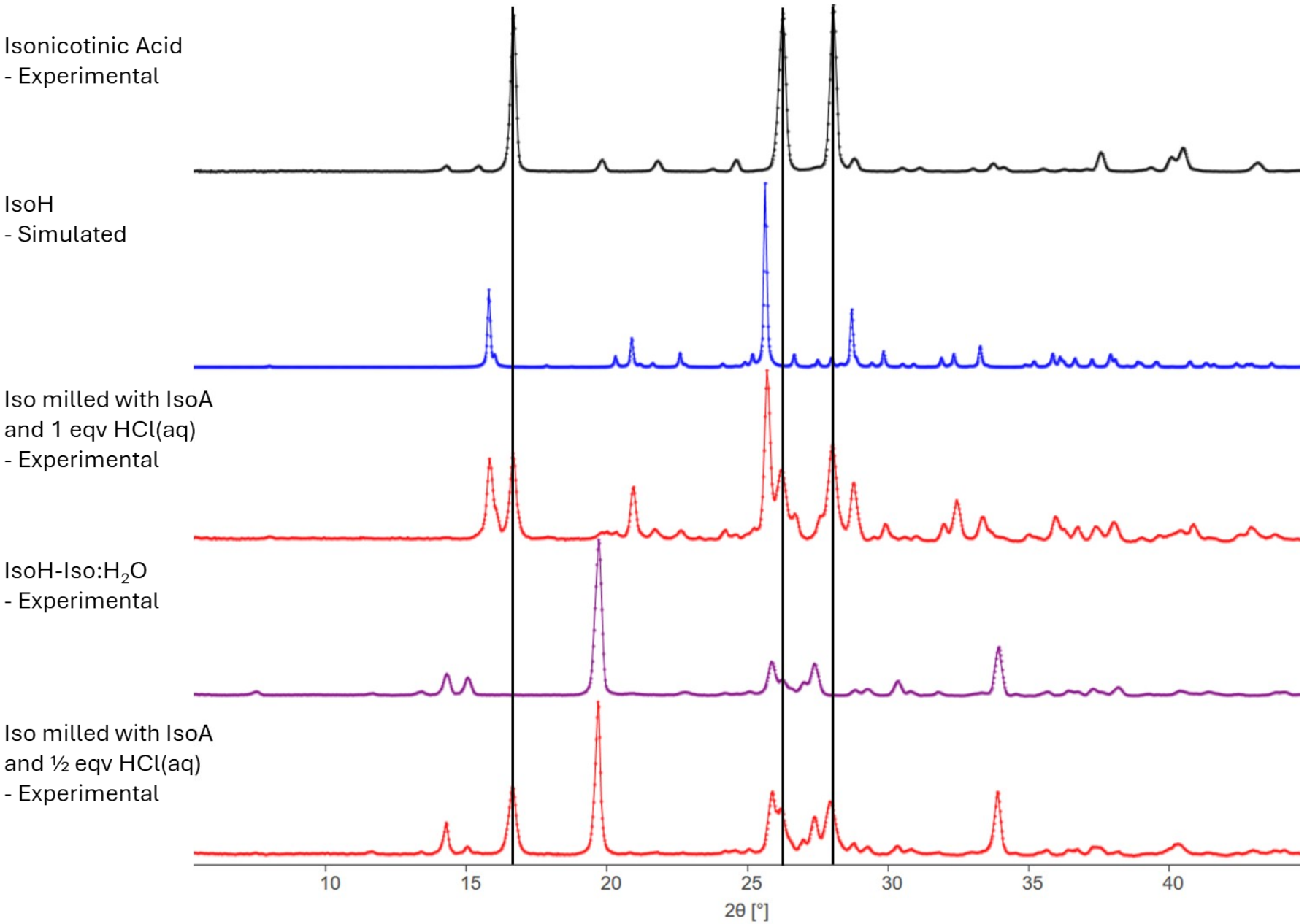

Fig. S9. PXRD patterns of **IsoA**, **IsoH**, and **IsoH-Iso:H_2O** and competitive milling reactions between **Iso** and **IsoA**.

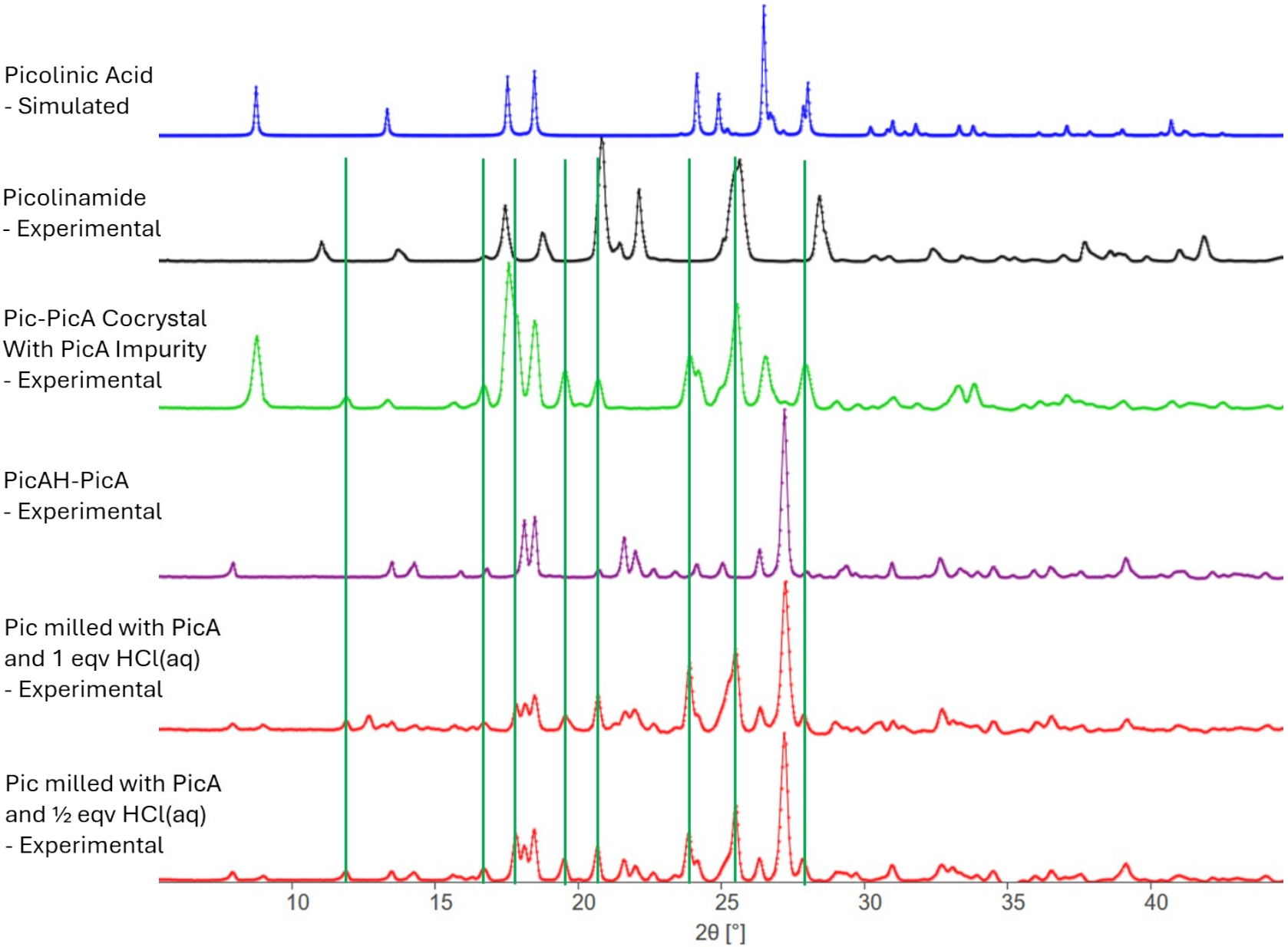

Fig. S10. PXRD patterns of **Pic**, **PicA**, **Pic-PicA**, **PicAH-PicA** and competitive milling reactions between **Pic** and **PicA**.

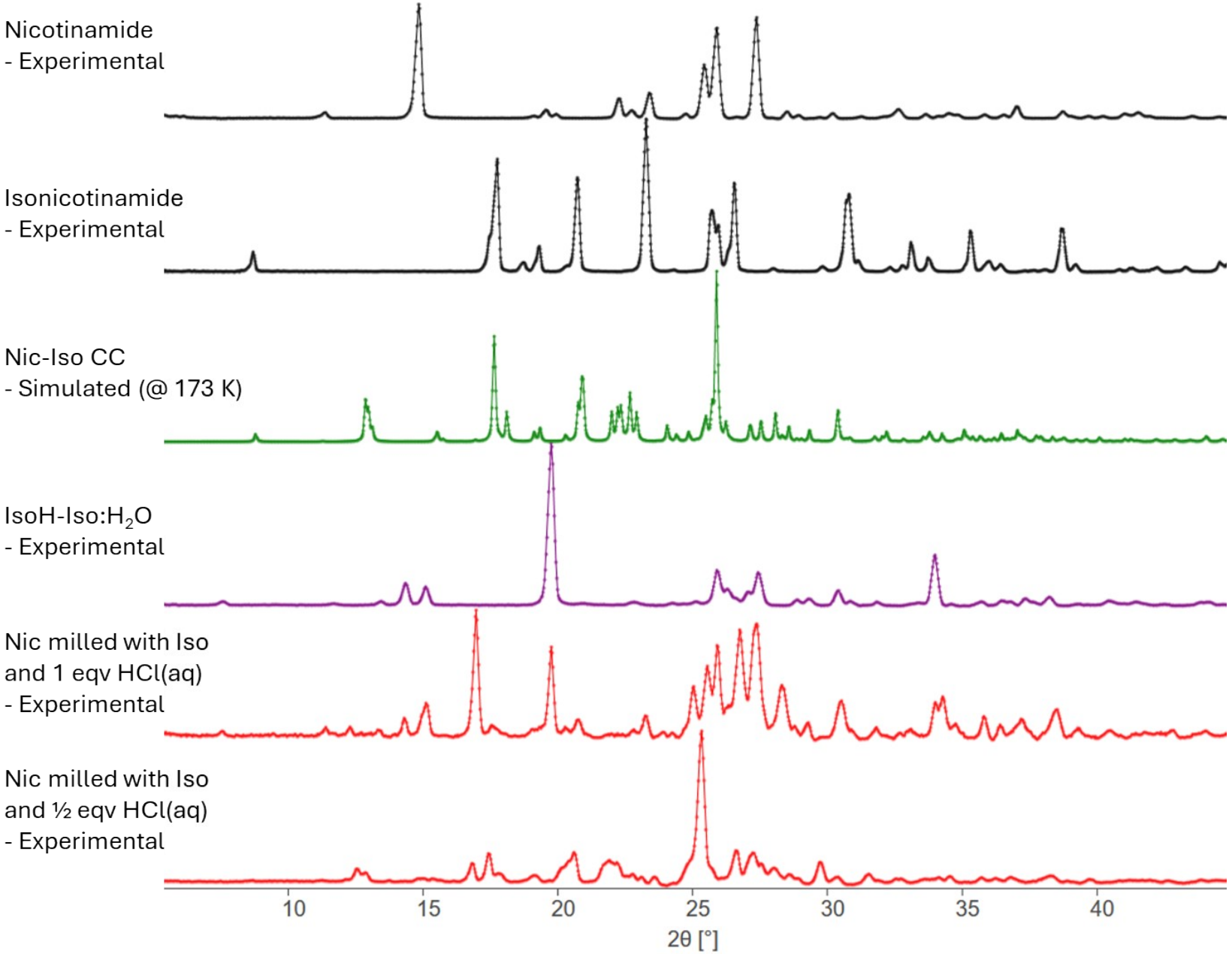

Fig. S11. PXRD patterns of **Nic**, **Iso**, **Nic-Iso**, **IsoH-Iso:H_2O** and competitive milling reactions between **Nic** and **Iso**.

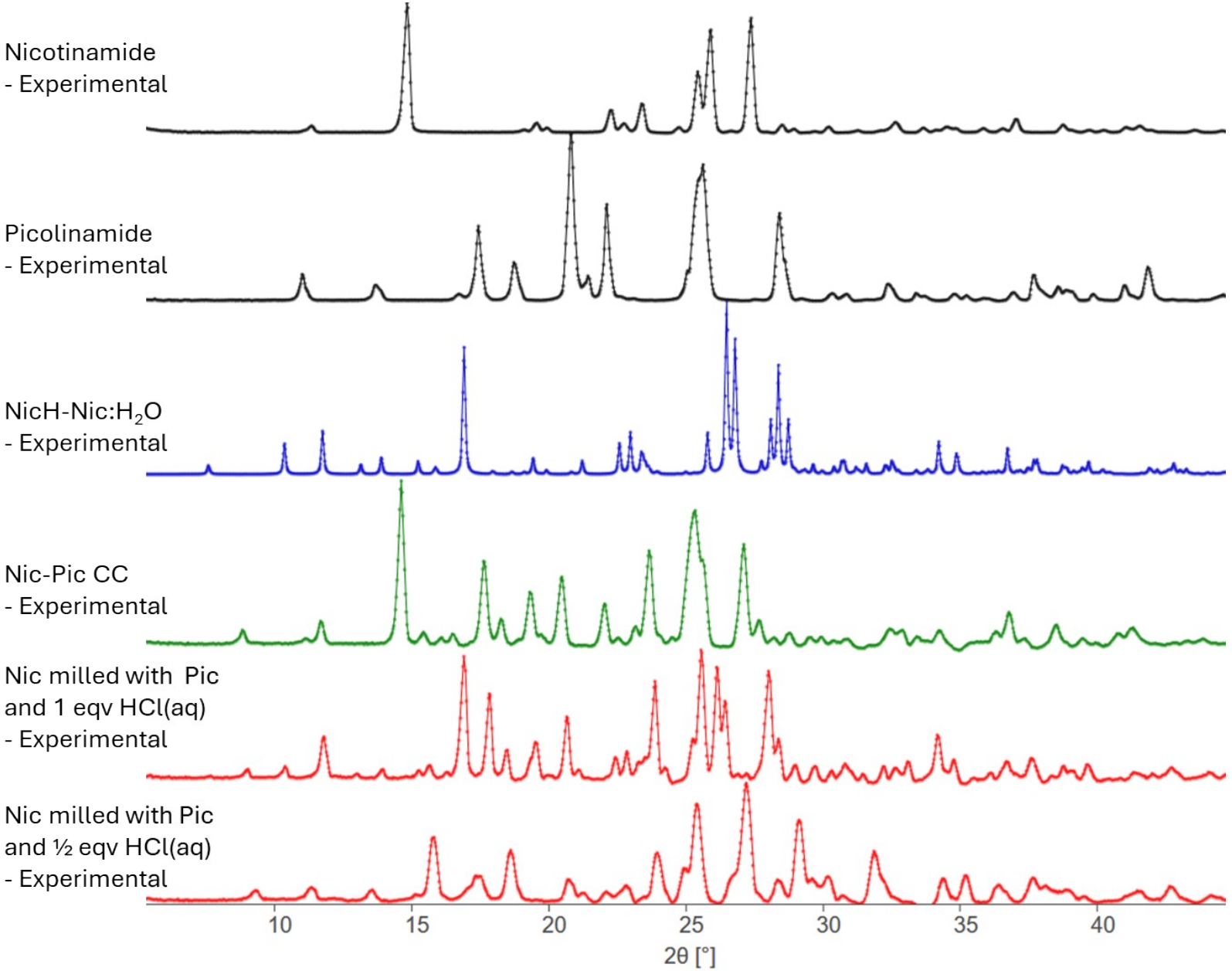

Fig. S12. PXRD patterns of **Nic**, **Pic**, **NicH-Nic:H_2O**, **Nic-Pic**, and competitive milling reactions between **Nic** and **Pic**.

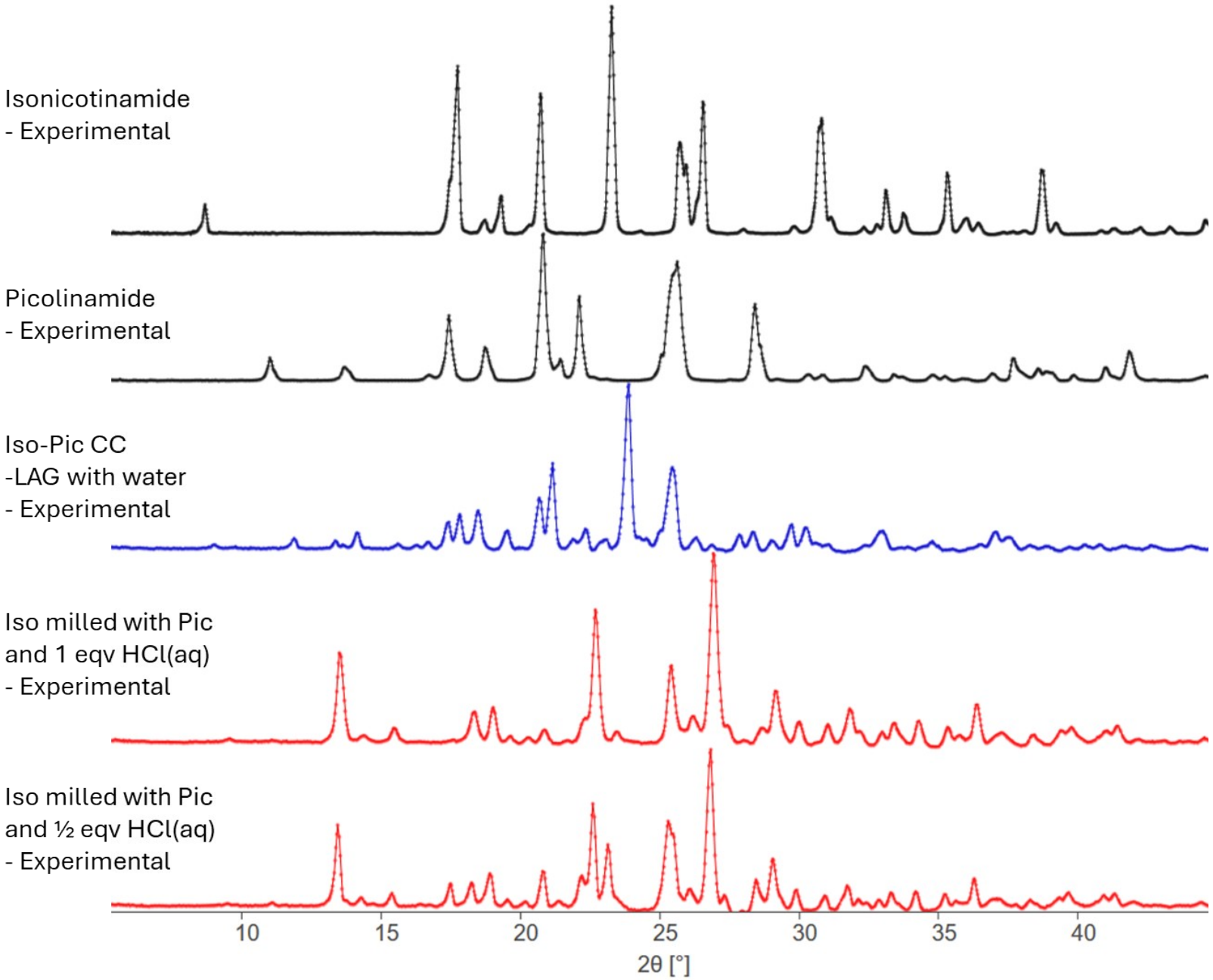

Fig. S13. PXRD patterns of **Iso**, **Pic**, **Iso-Pic**, and competitive milling reactions between **Iso** and **Pic**.

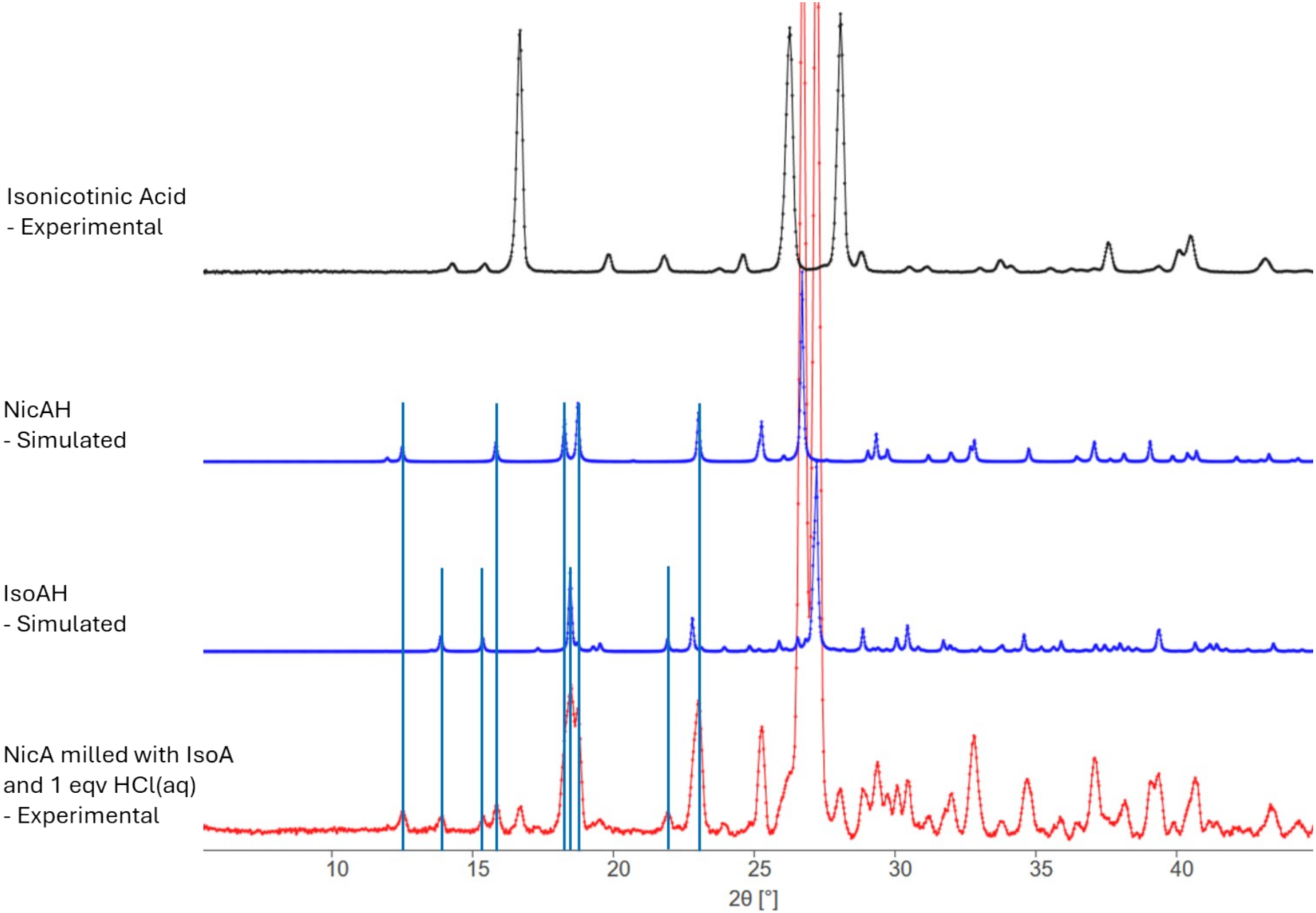

Fig. S14. PXRD patterns of **IsoA**, **NicAH**, **IsoAH**, and competitive milling reactions between **IsoA** and **NicA**.

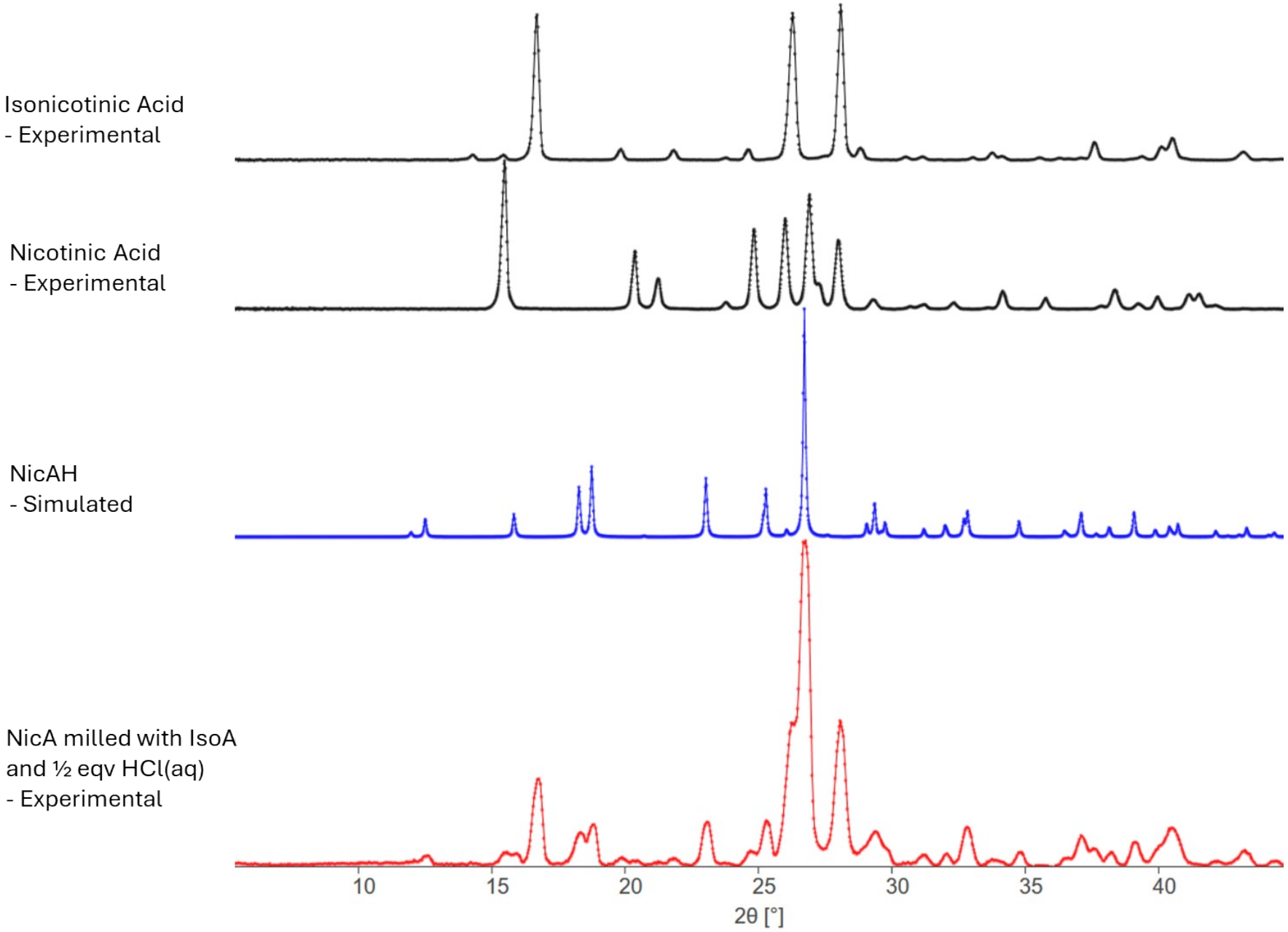

Fig. S15. PXRD patterns of **IsoA**, **NicA**, **NicAH**, and competitive milling reactions between **IsoA** and **NicA**.

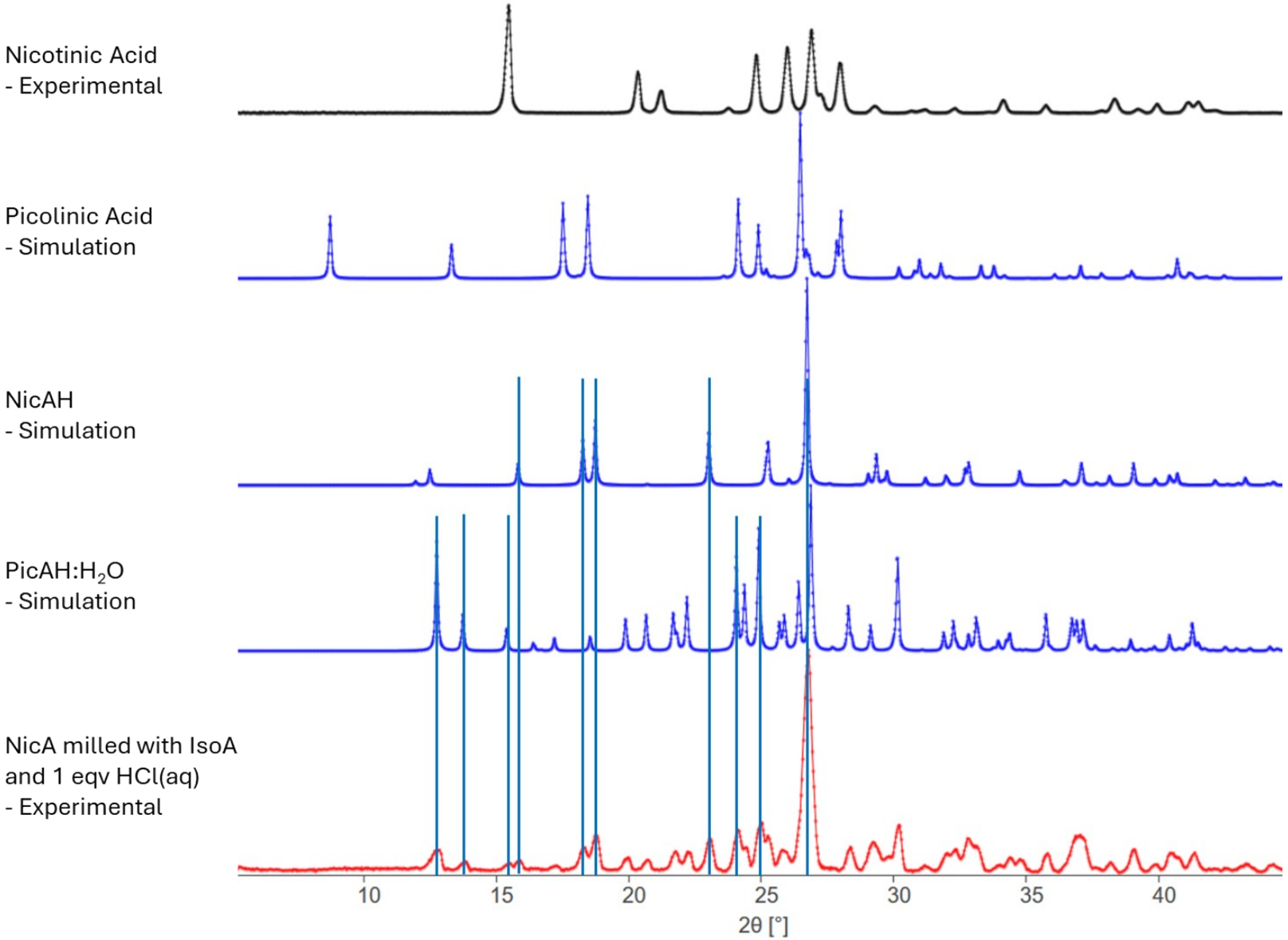

Fig. S16. PXRD patterns of **NicA**, **PicA**, **NicAH**, **PicAH:H_2O** and competitive milling reactions between **PicA** and **NicA**.

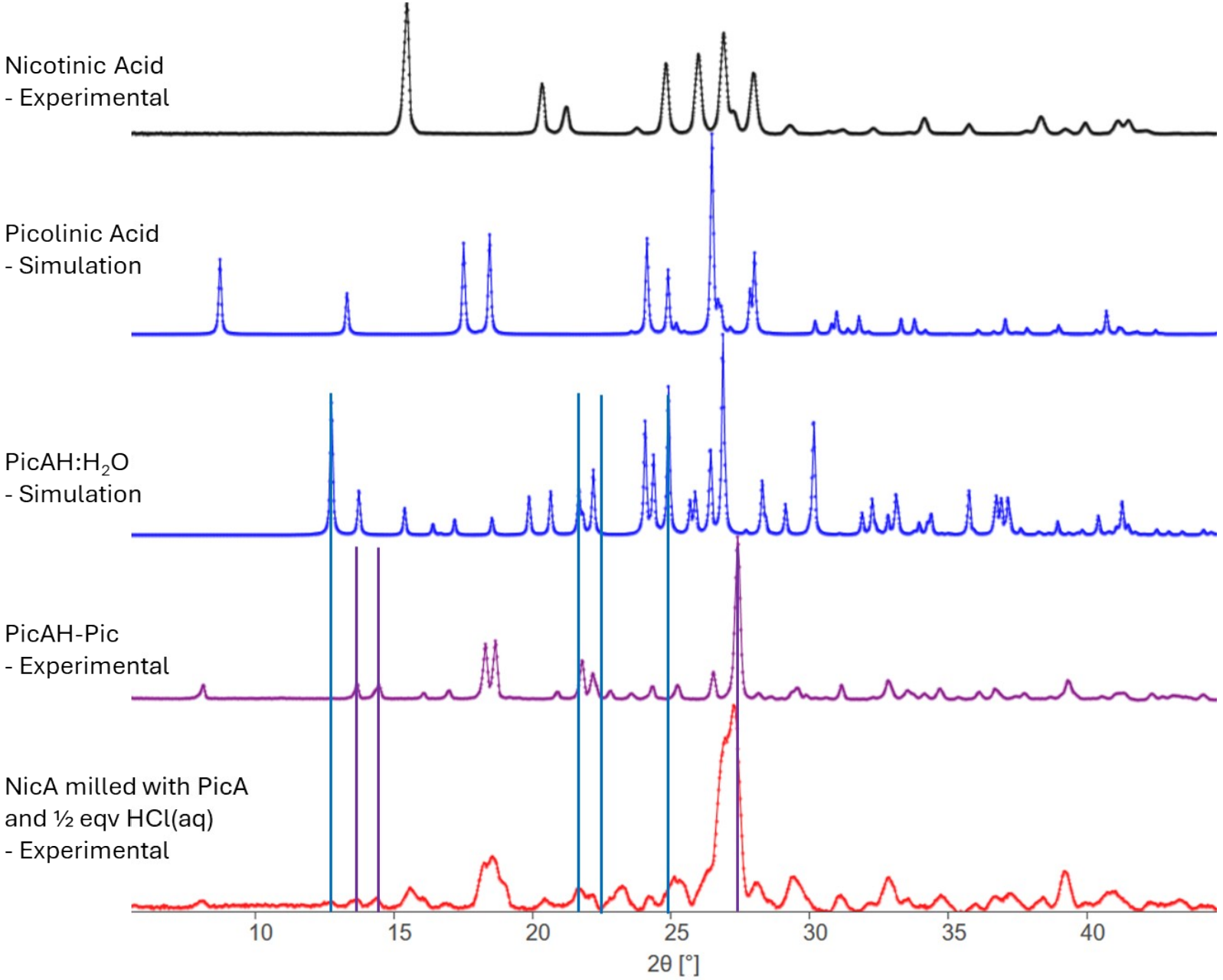

Fig. S17. PXRD patterns of **NicA**, **PicA**, **PicAH:H_2O**, **PicAH-Pic** and competitive milling reactions between **PicA** and **NicA**.

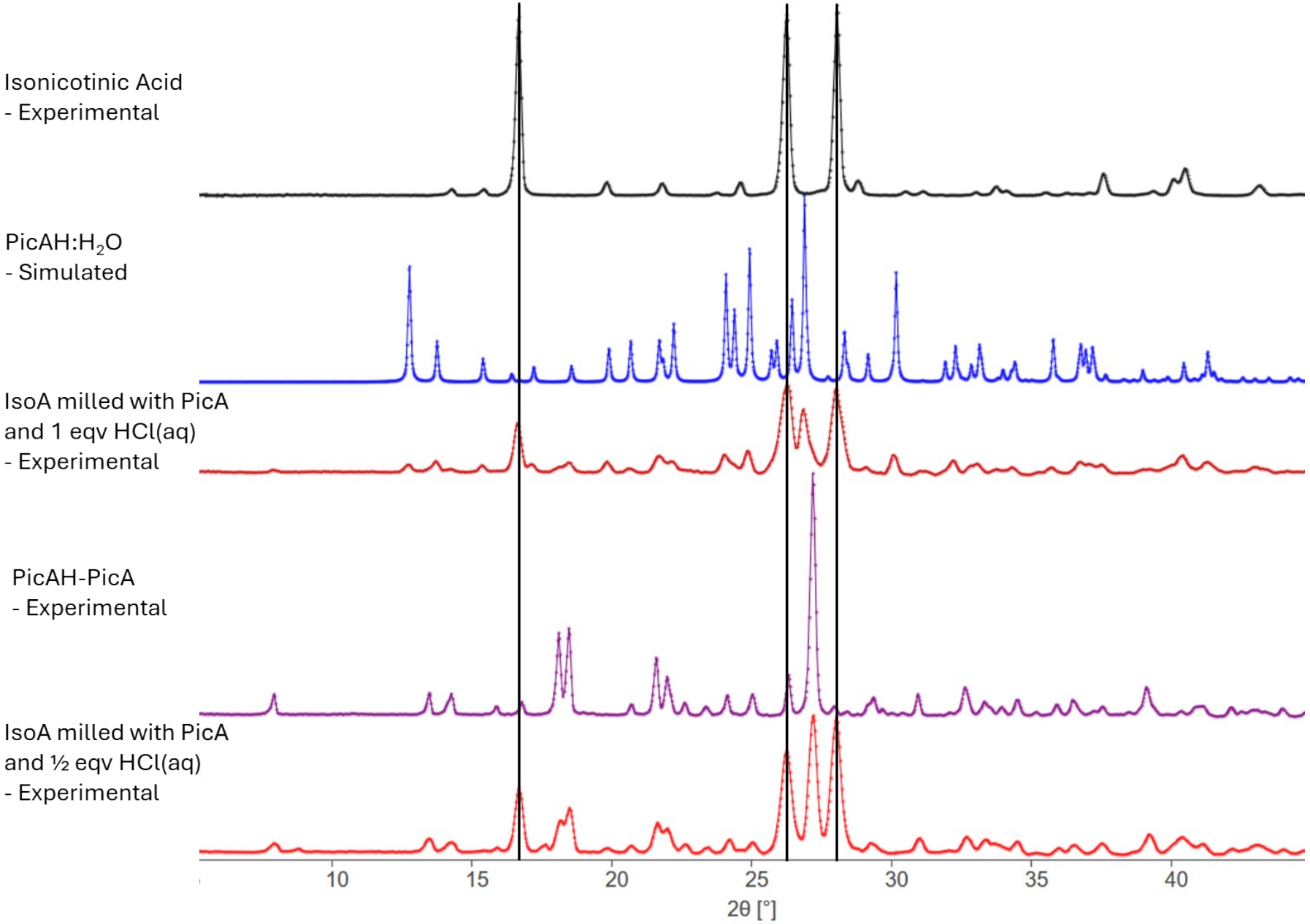

Fig. S18. PXRD patterns of **IsoA**, **PicA**, **PicAH:H_2O**, **PicAH-Pic** and competitive milling reactions between **PicA** and **IsoA**.

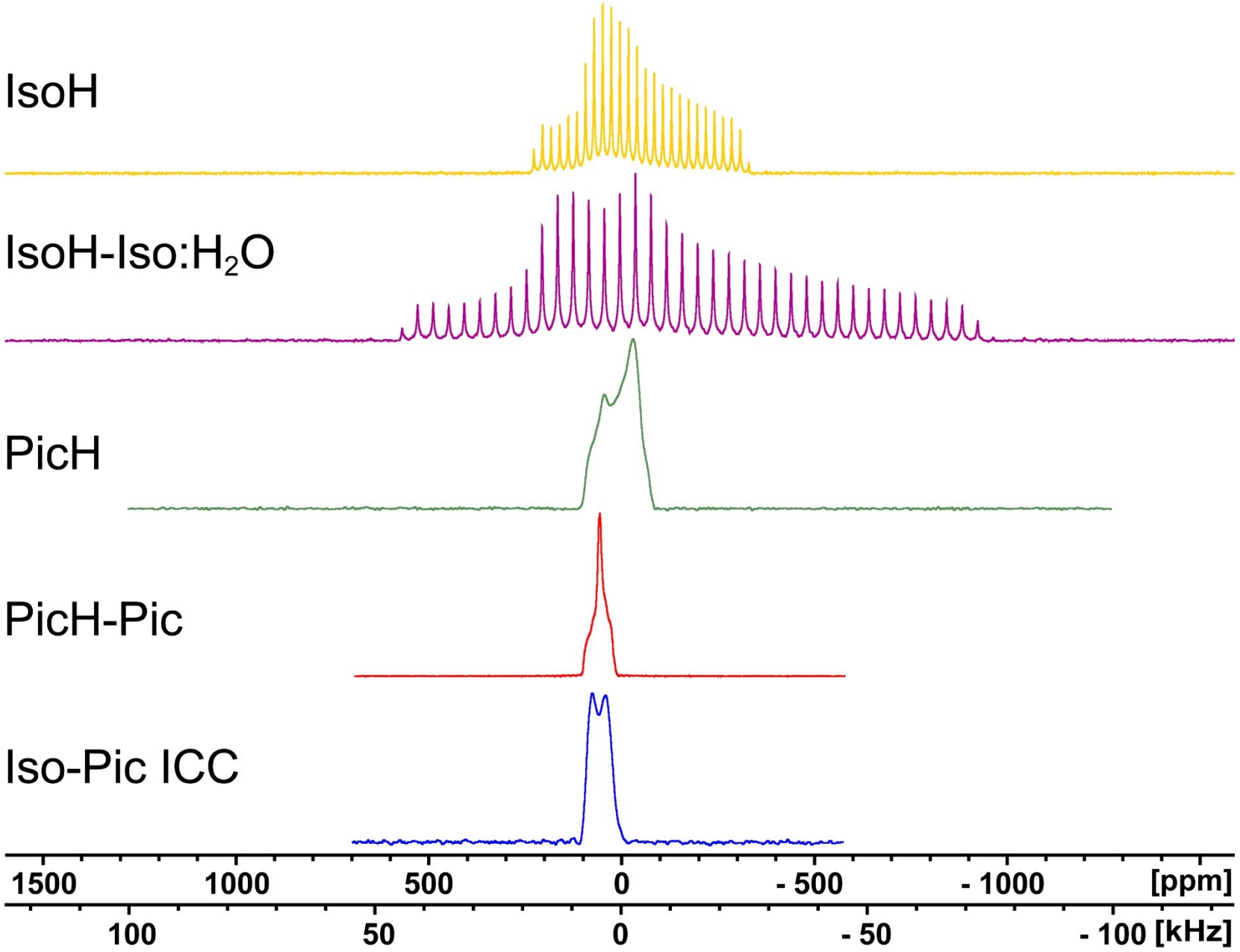

Fig. S19. ^{35}Cl static SSNMR of **IsoH**, **IsoH-Iso:H_2O**, **PicH**, **PicH-Pic**, and **Iso-Pic:HCl**.

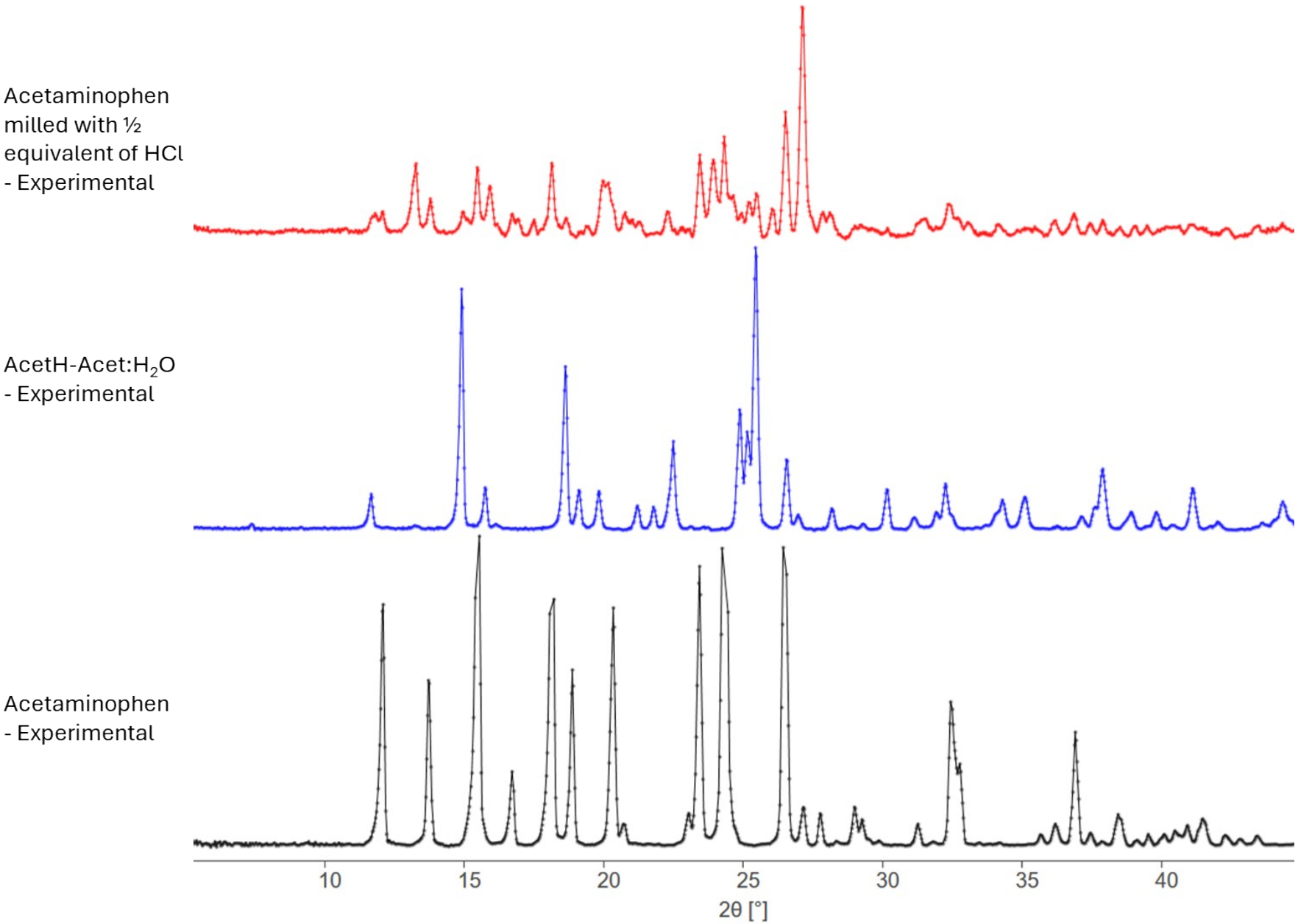

Fig. S20. PXRD patterns of **AcetH-Acet:H_2O**, **Acet**, and **Acet** milled with ½ equivalent of HCl(aq).

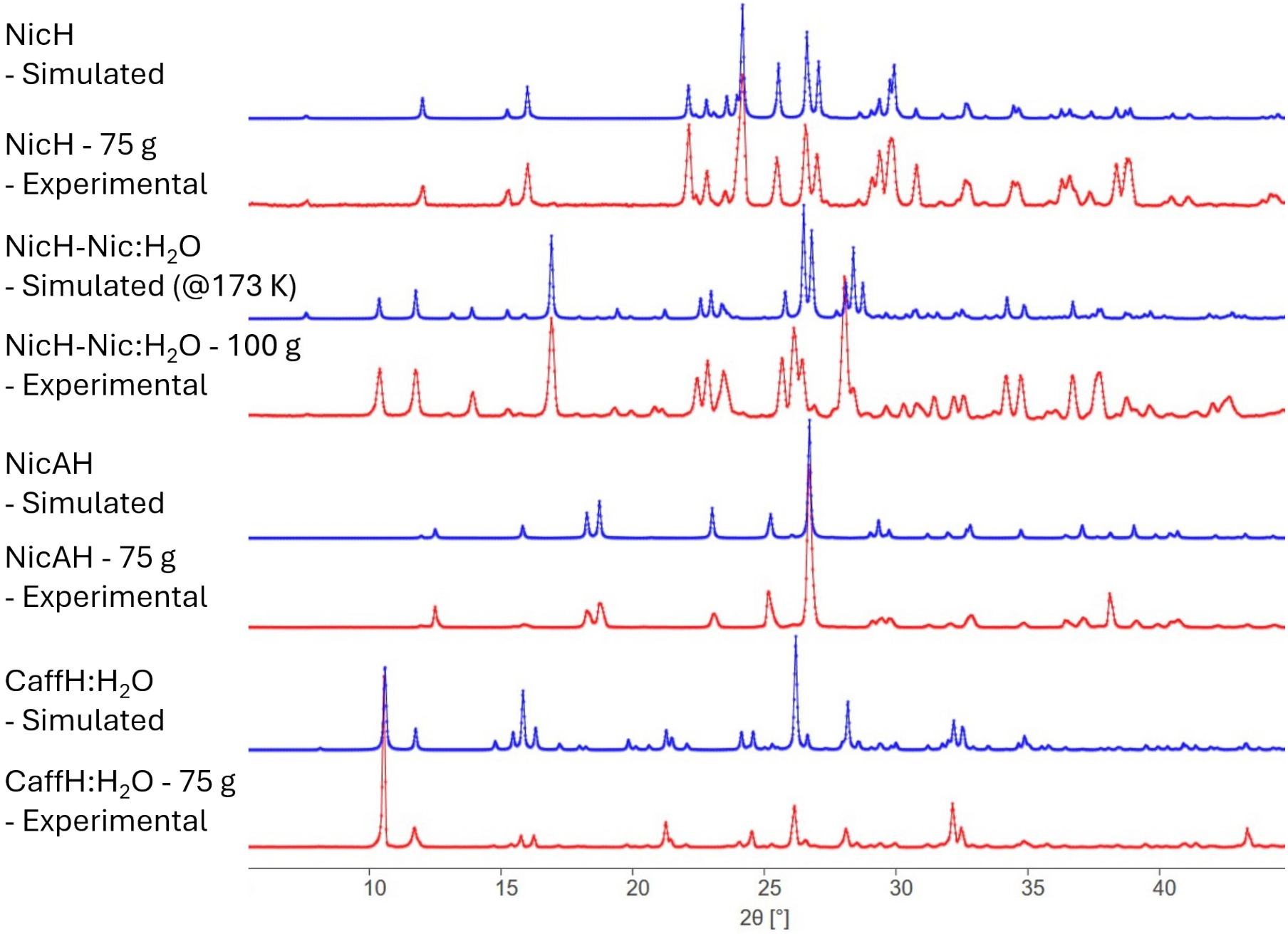

Fig. S21. PXRD patterns of scaled up reactions (red) compared to simulated patterns of various HCl salts (blue).

Table S6. Summary of results from SCXRD analysis of **PicH:H_2O**.

Empirical formula	$C_6H_9ClN_2O_2$
Formula weight	176.60
Temperature [K]	299(3)
Crystal system	monoclinic
Space group (number)	$P2_1/n$ (14)
a [Å]	7.33530(10)
b [Å]	8.04600(10)
c [Å]	14.1590(2)
α [°]	90
β [°]	96.8950(10)
γ [°]	90
Volume [Å^3]	829.618(19)
Z	4
ρ_{calc} [gcm^{-3}]	1.414
μ [mm^{-1}]	3.731
F(000)	368
Crystal size [mm^3]	0.21×0.136×0.043
Crystal color	clear whiteish colorless
Crystal shape	irregular
Radiation	Cu K_α (λ=1.54184 Å)
2θ range [°]	12.59 to 160.66 (0.78 Å)
Index ranges	$-7 \le h \le 9$ $-10 \le k \le 10$ $-18 \le l \le 18$
Reflections collected	16704
Independent reflections	1796 R_{int} = 0.0456 R_{sigma} = 0.0269
Completeness to θ = 67.684°	99.9 %
Data / Restraints / Parameters	1796/3/106
Goodness-of-fit on F^2	1.092
Final R indexes [$I \ge 2\sigma(I)$]	R_1 = 0.0359, wR_2 = 0.1007
Final R indexes [all data]	R_1 = 0.0375, wR_2 = 0.1027
Largest peak/hole [eÅ^{-3}]	0.31/-0.28

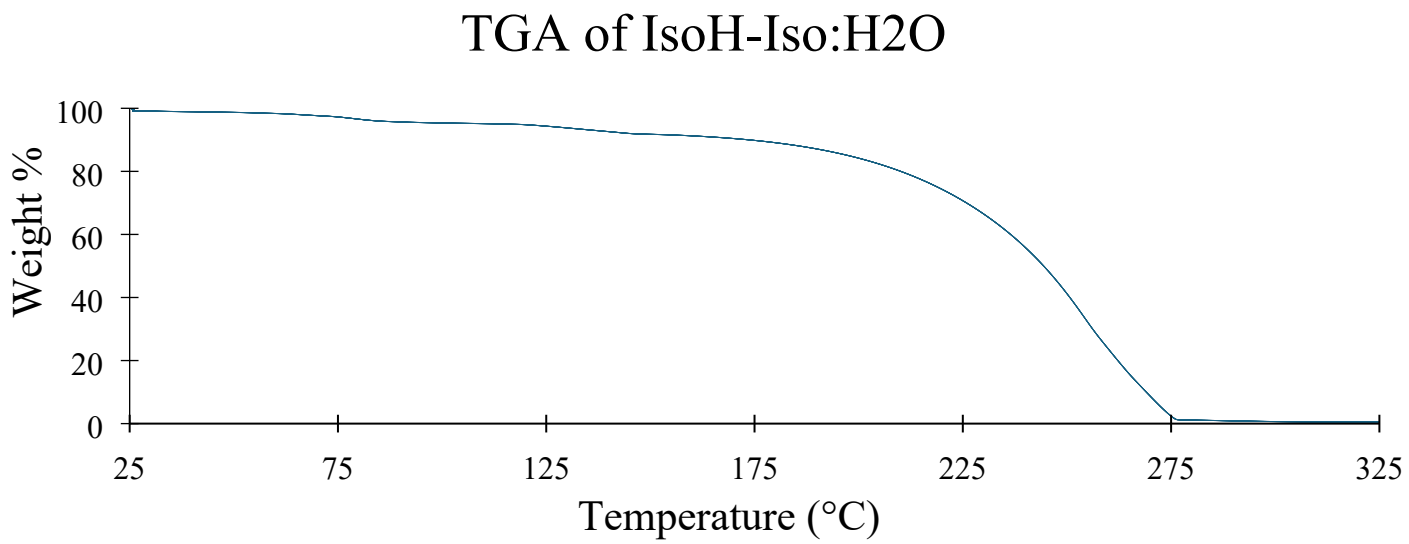

Fig. S22. TGA of **IsoH-Iso:H_2O** from 25 to 300 °C.

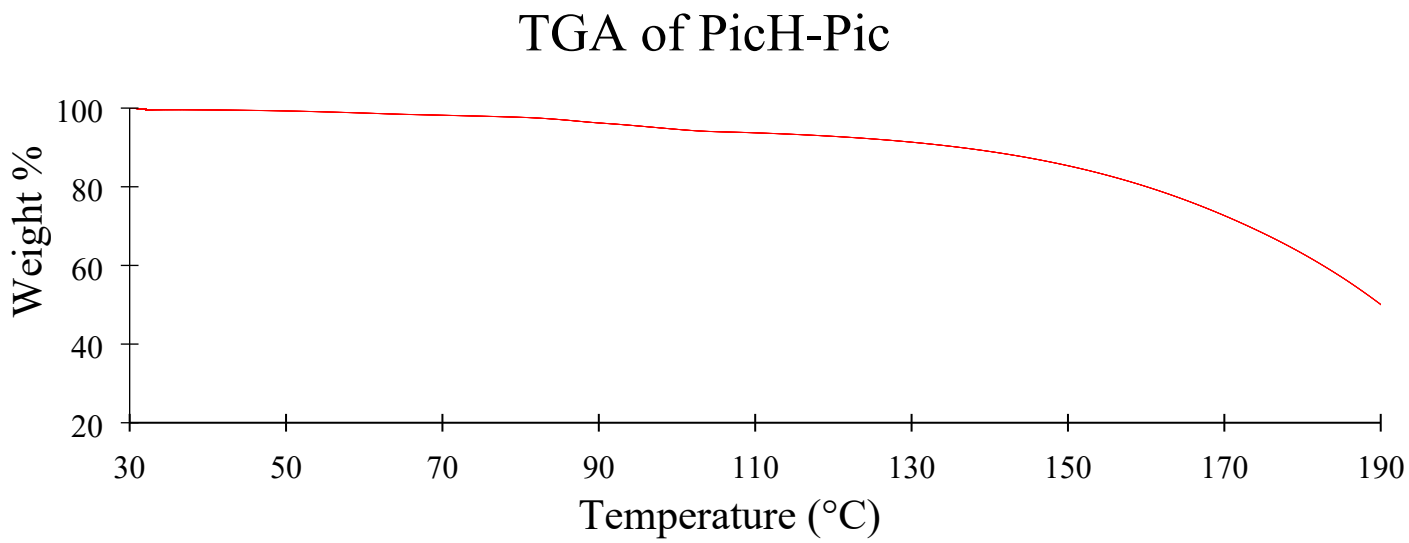

Fig. S23. TGA of **PicH-Pic** from 30 to 200 °C.

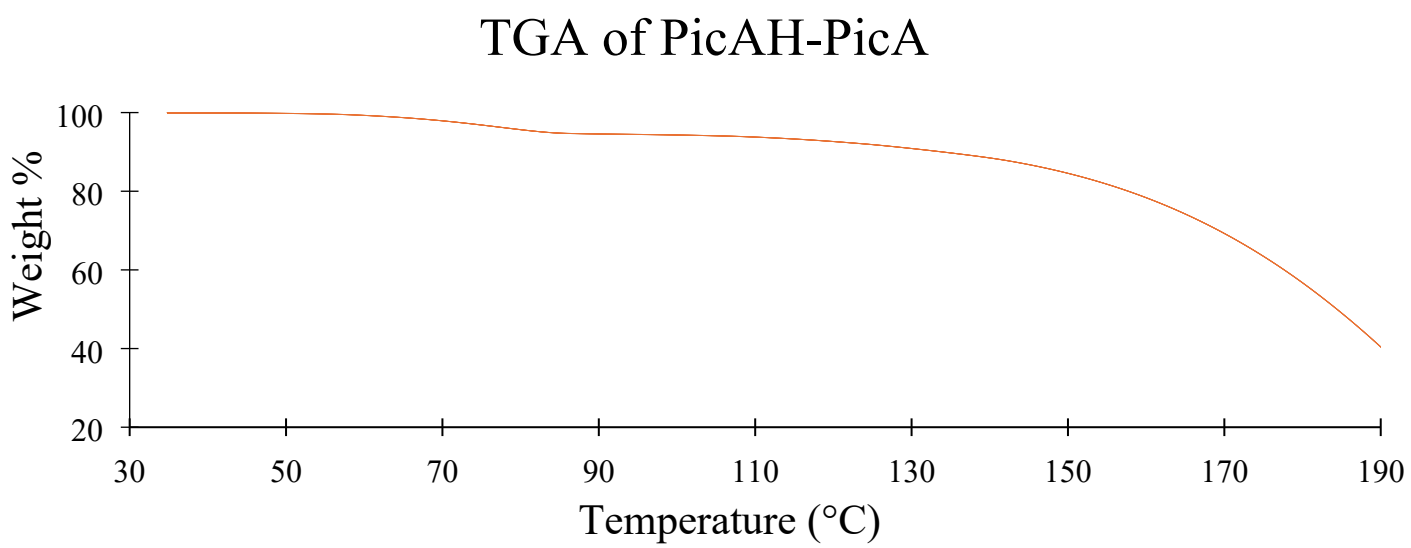

Fig. S24. TGA of **PicAH-PicA** from 30 to 200 °C.

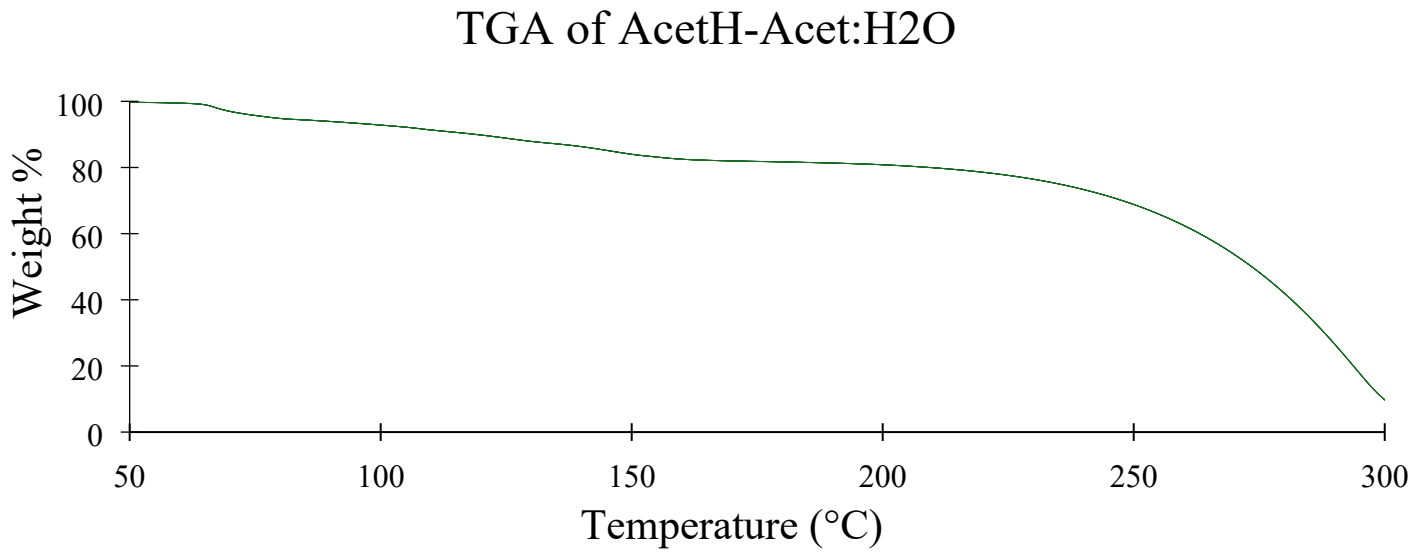

Fig. S25. TGA of **AcetH:Acet:H_2O** from 50 to 300 °C.

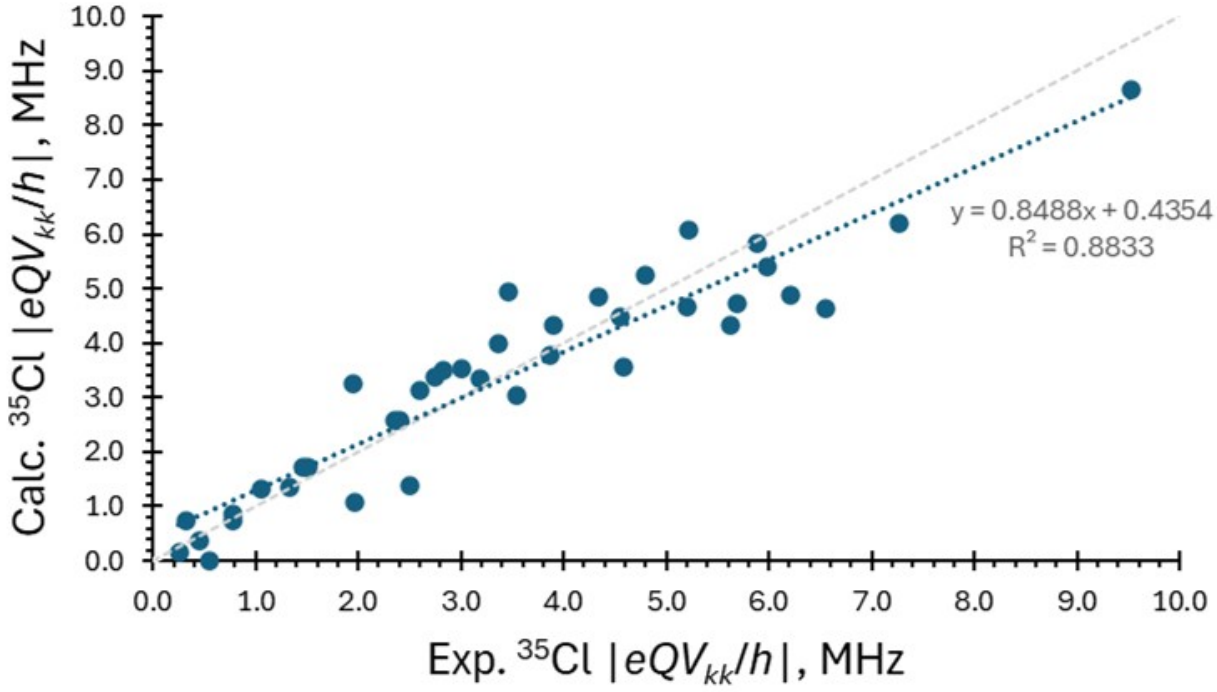

Fig. S26. Relationships between principal components of the ^{35}Cl EFG tensors were measured experimentally and calculated from DFT-D2* geometry optimized structures. The blue line represents the linear regression fit, while the grey line represents perfect correlation.

Supplement S1. The EFG distance and RMS EFG distance are metrics introduced by our laboratory[101] for assessing the agreement between experimental and calculated EFG tensors, and is used in a similar manner to the chemical shift distance and RMS chemical shift difference introduced by Alderman *et al* [*J. Magn. Reson*. **1993**, *101*, 188-197]. We assess the agreement between an experimental ($V_{kk}^{m,exp}$, k = 1, 2, 3) and calculated ($V_{kk}^{m,calc}$) EFG tensor at nucleus m using the EFG distance (Γ_m) metric. The EFG distance quantifies the degree of similarity between two sets of the principal components of EFG tensors (here, one experimental and one computed set of tensors) using a single scalar value:

$$\Gamma_m = \frac{eQ}{h}\left(\frac{1}{15}\left[3\Delta_{11}^2 + 3\Delta_{22}^2 + 3\Delta_{33}^2 + 2\Delta_{11}\Delta_{22} + 2\Delta_{11}\Delta_{33} + 2\Delta_{22}\Delta_{33}\right]\right)^{1/2}$$

$$\Delta_{kk} = \left|\left|V_{kk}^{m,calc}\right| - \left|V_{kk}^{m,exp}\right|\right|$$

In the above expressions, e is the elementary charge, h is Planck's constant, and Q is the nuclear quadrupole moment [$Q(^{35}\mathrm{Cl})$ = –8.165 fm^2]. A root-mean-square EFG distance for an ensemble of M EFG tensors (Γ_{RMS}) is determined by the following equation:

$$\Gamma_{RMS} = \left(\frac{1}{M}\sum_m \Gamma_m^2\right)^{1/2}$$

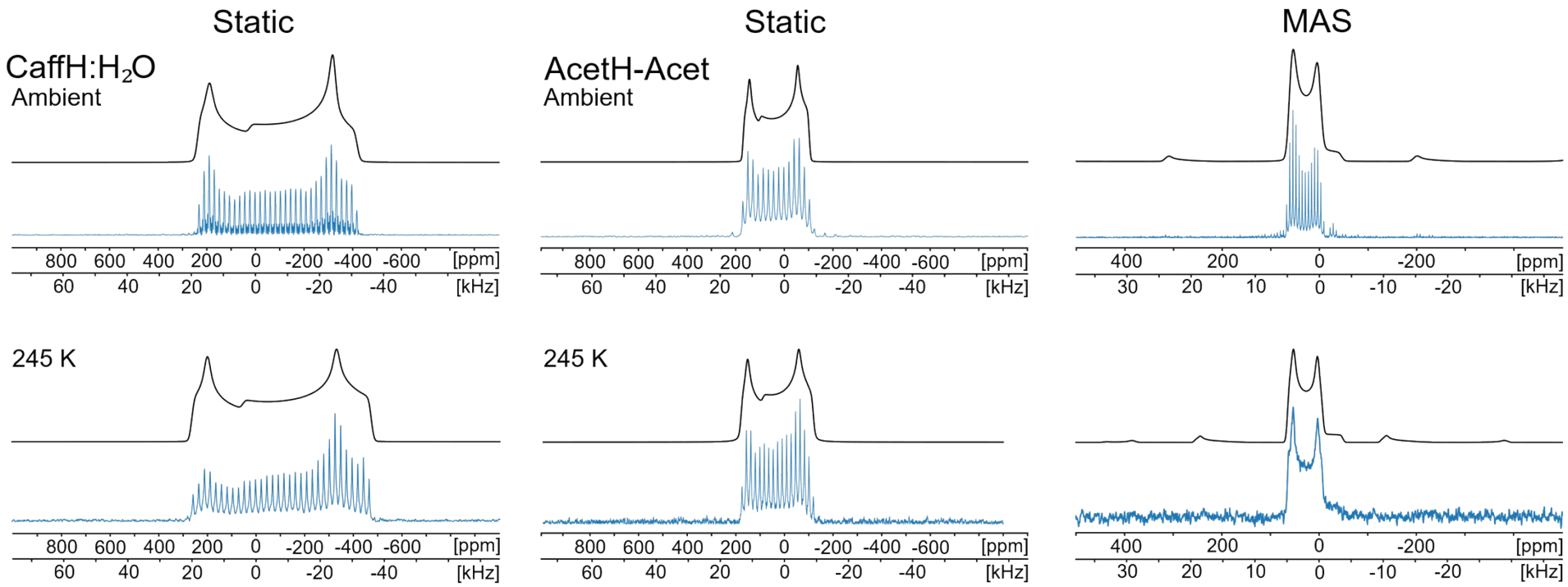

Fig. S27. Comparison of ^{35}Cl SSNMR spectra acquired at 18.8 T under ambient conditions and at 245 K for **CaffH:H$_2$O** and **AcetH-Acet**. At For **CaffH:H$_2$O** at 245 K: $C_Q = 5.6$ MHz, $\eta_Q = 0.16$, $\delta_{iso} = 11.1$ ppm. For **AcetH-Acet** at 245 K: $C_Q = 3.51$ MHz, $\eta_Q = 0.17$, $\delta_{iso} = 77.2$ ppm.